

# Fabrication and characterization of electrodeposited crystalline Au nanowires into anodic alumina templates

S. AGARWAL<sup>1</sup>, S. KUMAR<sup>2</sup>, M. S. KHATRI<sup>1,\*</sup>

<sup>1</sup>Department of Physics, National Institute of Technology, Uttarakhand, India

<sup>2</sup>Department of Applied Sciences, Punjab Engineering College, Chandigarh, India

Gold nanowires were fabricated using three electrode arrangements by electrodeposition method. Conducting alumina templates were used as a working electrode and platinum wire as the counter electrode. Formation of gold nanowires has been evidenced using characterization techniques such as X-ray diffraction (XRD) and scanning electron microscopy (SEM). It was found by cross-sectional SEM micrograph that the average length of nanowires is  $\sim 800$  nm. The presence of four characteristic peaks at  $2\theta$  value of  $37.89^\circ$ ,  $44.06^\circ$ ,  $64.46^\circ$ ,  $77.36^\circ$  and  $81.54^\circ$  corresponding to (111), (200), (220) (311) and (222) planes have confirmed the crystalline nature of nanowires. I–V measurements of gold nanowires have shown typical metallic characteristics after post deposition annealing at  $200^\circ\text{C}$ . The small non-linear regions observed in I–V measurements are attributed to the presence of defects in nanowires. The impedance behavior of nanowires was recorded using impedance analyzer. The decrease in impedance after 0.10 MHz is due to high capacitive coupling resulting from very high pore density of the alumina template.

(Received May 26, 2021; accepted April 8, 2022)

Keywords: Au nanowires, Electrodeposition, Alumina oxide template, Nanomaterial

## 1. Introduction

Over the last one decade the fabrication of nanomaterials for their potential technological applications have represented one of the most attractive interdisciplinary science researches. The growing interest in the field of nanomaterials is due their applications in chemical industry, fuel cell, batteries, sensors, and in electronics devices [1-4]. There are several techniques available for the preparation of nanomaterials [5-8]. The synthesis of nanodots or nanowires (NWs) into nano porous alumina template via electrodeposition technique is a simple, economic and high yield technique [9]. Porous anodic alumina oxide (AAO) is mechanically strong, optically translucent and electrically insulating in nature [10,11]. It is one of the most promising membrane for fabrication of nanostructures due to its simple and self-organized porous morphology. AAO is formed in a self-organized process on the surface of aluminum in a self-organized manner when anodized in an acid bath such as sulphuric acid, oxalic acid, phosphoric acid or chromic acid under specific conditions [12]. The pore diameter and inter pore distance can be controlled by the fabrication conditions such as the electrolyte, anodizing time, temperature, and voltage.

The depth of nano-channels can exceed upto  $100\ \mu\text{m}$  which makes the anodic porous alumina one of the most suitable membrane with a high-aspect ratio and high pore density (about  $10^9$ - $10^{11}$  pores/ $\text{cm}^2$ ) [13]. These self-organized nano-membranes have recently emerged as an important method for the synthesis of nanowires and nanodots of a variety of materials, such as metals [14-16], alloys [17, 18] and multilayers [19].

The trend towards the miniaturization of electronic devices has increased the requirement of suitable

interconnects with higher metallic conductivity at the nano level. Owing to the resistance against oxidation and excellent electrical conductivity gold is an ideal interconnect material [20]. In comparison to the other nanostructures of gold, nanowires are suitable candidates as interconnects due to their one-dimensional geometry and superior conducting properties [21-23]. Such nanowires have also been used as elementary unit for sensing devices in the field of biology and life sciences because of their unusual optical, electrical and mechanical properties [24]. In this paper, we have shown how AAO template can be used for the fabrication of uniform and well aligned Au nanowires.

## 2. Experiment

Au nanowires were electrodeposited using three-electrode cell with a silver chloride (Ag/AgCl) as the reference electrode and a platinum wire as the counter electrode. Aluminum oxide templates with pore diameter of  $\sim 100$  nm and a channel length of  $30\ \mu\text{m}$  were used as a cathode for the deposition of nanowires. The deposition process is carried out at room temperature in a Teflon cell using gold sulfite electrolyte with three-electrode configuration and controlled by a Biologic SP-200 potentiostat. As electrodeposition requires the conducting substrate, therefore, thin layer of Au is deposited by sputtering method on one side of the alumina template. Thus, the Au coated alumina template acts as a working electrode during the deposition process.

X-ray diffractometer (Panalytical X'pert) using CuK $\alpha$  radiation ( $\lambda=1.5406\ \text{\AA}$ ) was used for structural characterization of gold nanowires embedded in AAO

measurements (XRD). The structure and microstructure of the nanowires were studied using LEO 1530 Gemini scanning electron microscope. Keysight B2912A source meter was used for electrical characterization of gold nanowires. Sample was coated with silver paste on both sides of AAO prior to electrical characterization and then annealed at 200°C. Keysight E4990A Impedance Analyzer was used for recording the impedance behavior of gold nanowires. The impedance measurements were carried out on sample size of 5 mm x 3 mm.

### 3. Results and discussion

The deposition curves were recorded in an electrolyte at a constant potential of -0.8 V with reference to the Ag/AgCl electrode. The current transient plot is shown in Fig. 1 for deposition of Au nanowires. At the onset of region I, the concentration of gold ions at the base of the pores and adjacent to the working electrode is comparable to the bulk concentration of the electrolyte and the reaction is determined by charge transfer mechanism. It is observed that current rapidly decreases because of the beginning of mass transport process which is accompanied by expansion of the diffusion layer into the electrolyte (region I). It is found from the current-transient curve in Fig. 1 that after the initial decrease due to deficiency of metal ions within the pores of the template, the deposition current is almost constant during the filling of the pores (region II) [25].

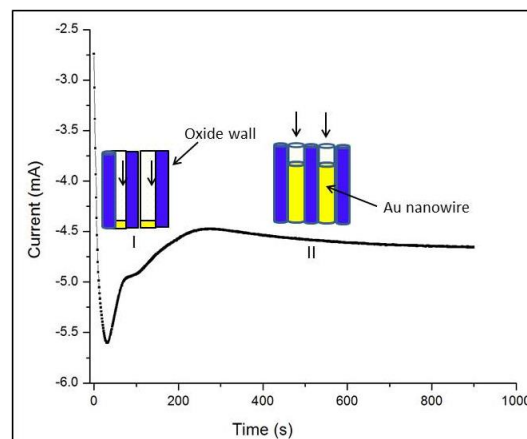


Fig. 1. Current-time ( $I-t$ ) curve for the growth of Au nanowires during different stages of electrodeposition. The growth of Au nanowires (yellow cylinders) is schematically depicted (color online)

Fig. 2 (a, b and c) shows the cross-sectional SEM morphology of Au nanowires. The images are taken by breaking the templates and are recorded at the cross-section of the AAO template. The cross-sectional micrographs show the formation of uniform cylindrical nanowires standing freely on gold substrate. The scale bar of known length as shown at the bottom of the SEM micrograph is used to estimate the length and diameter of nanowires. These nanowires have the average diameter and length of  $\sim 100$  nm and  $\sim 800$  nm, respectively.

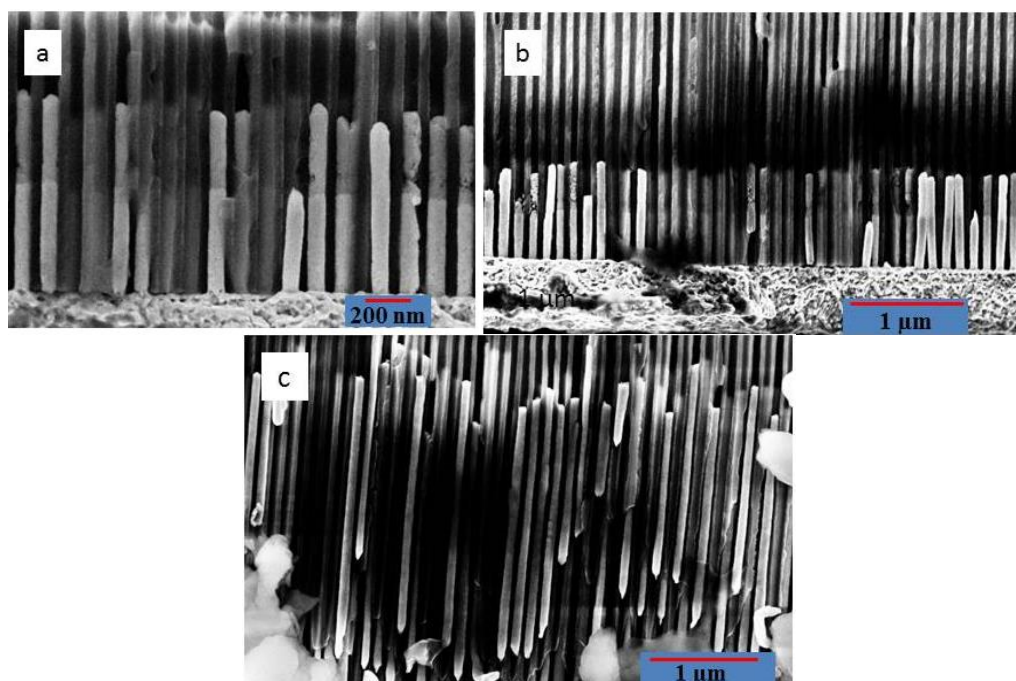


Fig. 2 (a), (b) and (c) cross-sectional SEM micrographs after electrodeposition shows nanowires embedded inside the pores of AAO alumina templates (color online)

XRD pattern of the gold nanowires is depicted in Fig. 3 with  $2\theta$  values between  $30^\circ$  and  $90^\circ$ . The XRD pattern of gold nanowires in Fig. 3 shows four characteristic peaks for  $2\theta$  at  $37.89^\circ$ ,  $44.06^\circ$ ,  $64.46^\circ$ ,  $77.36^\circ$  and  $81.54^\circ$  correspond

to (111), (200), (220) (311) and (222) set of planes, respectively (with reference to JCPDS File no. 04-0784). A pronounced (111) diffraction peak suggests a preferred growth of nanowires along (111) planes. Thus, the XRD

pattern clearly demonstrates that the gold nanowires synthesized by the electrodeposition method are crystalline in nature.

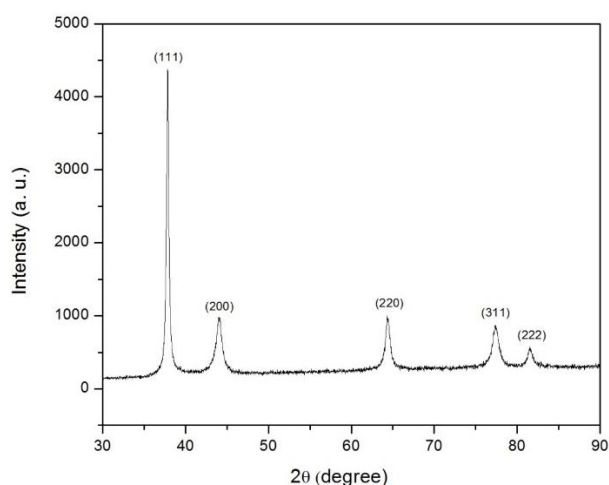


Fig. 3. X-ray diffraction pattern of gold nanowires embedded into AAO template.

Fig. 4 depicts the I–V characteristics of as deposited gold nanowires annealed at 200°C. It is observed that there is a linear increase in current with rise of voltage as normally occurs in metals. We have repeated the experiment three times under same conditions. Conduction in metals is more reliant on electron scattering at grain boundaries and the surface of embedded nanowires in AAO. The high aspect ratio nanowires will lead to the presence of a greater number of unbounded atoms lying at the surface due to large surface area to volume ratio. This results in a greater number of defects at the surface of nanowires. Due to such defects, electron scattering occurs results in small non-linear regions. It is also observed that the resistance is more in reverse biasing as compared to forward biasing. Such as synthesized gold nanowires may be useful as interconnects in futuristic nanodevices [26].

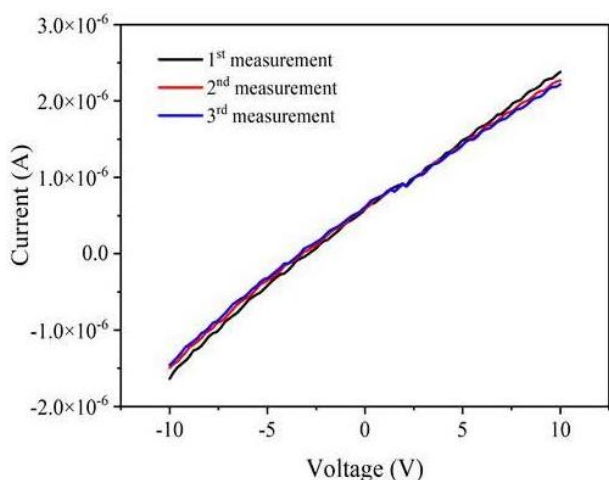


Fig. 4. Current-voltage (I–V) behaviour of as synthesized Au nanowires recorded three times under similar conditions (color online)

Impedance measurement of gold nanowires deposited into the pores of alumina template with varying frequency (from 80 kHz to 5 MHz) is shown in Fig. 5. Decrease in impedance after 0.10 MHz is clearly depicted in Fig. 5. Observed decrease in impedance may be credited to high capacitive coupling at higher frequencies [27]. The smaller inter pore distance results into very high pore density. This may be one of the reasons behind high capacitive coupling.

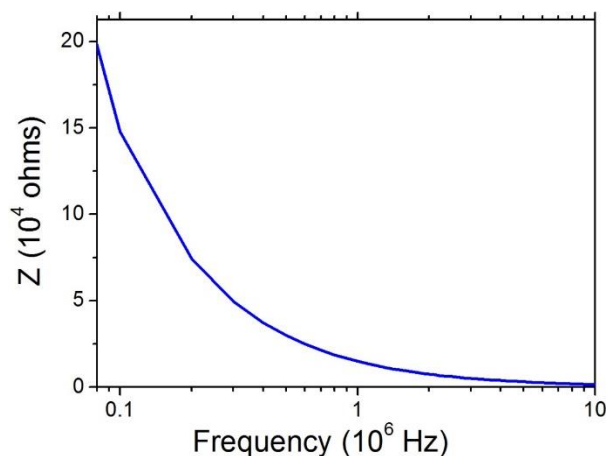


Fig. 5. Impedance response of gold nanowires deposited into the pores AAO templates (color online)

#### 4. Conclusion

Au coated anodic alumina oxide templates were used for the deposition of gold nanowires. Cross-sectional SEM micrographs have shown the formation of very uniform and continuous nanowires with the average length and diameter of  $\sim 800$  nm and 75 nm, respectively. Crystalline structure of gold nanowires is confirmed by X-ray diffraction measurements. I–V characteristics of as deposited nanowires annealed at 200°C have shown that there is a linear increase in current with rise of voltage. The small non-linear regions observed in current-voltage measurements are due to the existence of defects in nanowires. The drop in impedance of gold nanowires after 0.10 MHz is due to the high capacitive coupling at higher frequencies. Such gold nanowires are potential candidates as interconnects and elementary units for sensing devices in the field of biology and life sciences.

#### Acknowledgments

One of the authors Shivani Agarwal would like to acknowledge NIT Uttarakhand for providing her fellowship during the PhD programme.

#### References

- [1] Y. Li, J. Gong, G. He, Y. Deng, Mater. Chem. Phys. **134**, 1172 (2012).
- [2] H. Cui, C. Hong, A. Ying, X. Yang, S. Ren, ACS

- Nano **7**, 7805 (2013).
- [3] T. Adam, U. Hashim, Biosens. Bioelectron. **67**, 656 (2015).
- [4] S. Kundu, J. Mater. Chem. C **1**, 831(2013).
- [5] T. Guo, G. Yu, Y. Zhang, H. Xiang, F. Chang, C.-J. Zhong, J. Phys. Chem. C **121**, 3108 (2017).
- [6] C. E. Cross, J. C. Hemminger, R. M. Penner, Langmuir **23**, 10372 (2007).
- [7] S. Navaladian, C. M. Janet, B. Viswanathan, T. K. Varadarajan, R. P. Viswanath, Phys. Chem. C **111**, 14150 (2007).
- [8] F. Kim, K. Sohn, J. Wu, J. Huang, J. Am. Chem. Soc. **130**, 44 14442 (2008).
- [9] H. Zeng, M. Zheng, R. Skomski, D. J. Sellmyer, Y. Liu, L. Menon, S. Bandyopadhyay, J. Appl. Phys. **87**, 4718 (2000).
- [10] G. E. Thompson, Thin Solid Films **297**, 192 (1997).
- [11] H. Masuda, H. Yamada, M. Satoh, H. Asoh, Appl. Phys. Lett. **71**, 2770 (1997).
- [12] V. Sadasivan, C. P. Richter, L. Menon, P. F. Williams, AIChE J, **51**, 649 (2005).
- [13] G. D. Sulka, L. Zaraska, W. J. Stepniowski, Encyclopedia of Nanoscience and Nanotechnology **11**, 2<sup>nd</sup> ed. American Scientific: California, pp. 261-349, 2011.
- [14] H. Zeng, S. Michalski, R. D. Kirby, D. J. Sellmyer, L. Menon, S. Bandyopadhyay, Journal of Physics: Condensed Matter **14**, 715 (2002).
- [15] I. Dobosz, W. Gumowska, M. Czapkiewicz, J. Solid State Electrochem. **18**, 2963 (2014).
- [16] S. Kumar, S. Kumar, R. Kumar, S. K. Chakarvarti, Journal of Materials Science **39**, 2951 (2004).
- [17] T. R. Gaoa, L. F. Yina, C. S. Tiana, M. Lub, H. Sangb, S. M. Zhou Journal of Magnetism and Magnetic Materials **300**, 471 (2006).
- [18] H. Wang, E. Jia, L. Zhang, L. Li, M. Li, Physics Letters A **372**, 5712 (2008).
- [19] S. Agarwal, S.A. Hashmi, B. Nandan, A. K. Patra, R. P. Singh, J. A. Chelvane, M. S. Khatri, Chemical Physics Letters **684**, 378 (2017).
- [20] K. Critchley, B. P. Khanal, M. Grzny, L. Vigderman, S. D. Evans, E. R. Zubarev, N. A. Kotov, Advanced Materials **22**, 2338 (2010).
- [21] V. Rodrigues, T. Fuhrer, D. Ugarte, Phys. Rev. Lett. **85**, 4124 (2000).
- [22] D. Azulai, T. Belenkova, H. Gilon, Z. Barkay, G. Markovich, Nano Letters **9**, 4246 (2009).
- [23] A. Roy, T. Pandey, N. Ravishankar, A. K. Singh, AIP Advances **3**, 032131-1 (2013).
- [24] Q. Wang, F.Min, J. Zhu, Materials Letters **91**, 9 (2013).
- [25] J. Mallet, K. Yu-Zhang, C. L. Chien, T. S. Eagleton, P. C. Searson, Appl. Phys. Lett. **84**(19), 3900 (2004).
- [26] D. Saini, R. P. Chauhan, S. Kumar, J. Mater. Sci.: Mater. Electron **25**, 124 (2014).
- [27] S. Kumar, D. Saini, G. S. Lotey, N. K. Verma, Superlattices and Microstructures **50**(6), 698 (2011).

---

\* Corresponding author: mskhatri@gmail.com